

High-resolution morphological and biochemical imaging of articular cartilage of the ankle joint at 3.0 T using a new dedicated phased array coil: in vivo reproducibility study

Goetz H. Welsch · Tallal C. Mamisch · Michael Weber · Wilhelm Horger · Klaus Bohndorf · Siegfried Trattnig

Received: 20 November 2007 / Revised: 22 January 2008 / Accepted: 3 February 2008 / Published online: 12 April 2008
© ISS 2008

Abstract

Objective The objective of this study was to evaluate the feasibility and reproducibility of high-resolution magnetic resonance imaging (MRI) and quantitative T2 mapping of the talocrural cartilage within a clinically applicable scan time using a new dedicated ankle coil and high-field MRI. **Materials and methods** Ten healthy volunteers (mean age 32.4 years) underwent MRI of the ankle. As morphological sequences, proton density fat-suppressed turbo spin echo (PD-FS-TSE), as a reference, was compared with 3D true fast imaging with steady-state precession (TrueFISP). Furthermore, biochemical quantitative T2 imaging was prepared using a multi-echo spin-echo T2 approach. Data analysis was performed three times each by three different observers on sagittal slices, planned on the isotropic 3D-

TrueFISP; as a morphological parameter, cartilage thickness was assessed and for T2 relaxation times, region-of-interest (ROI) evaluation was done. Reproducibility was determined as a coefficient of variation (CV) for each volunteer; averaged as root mean square (RMSA) given as a percentage; statistical evaluation was done using analysis of variance.

Results Cartilage thickness of the talocrural joint showed significantly higher values for the 3D-TrueFISP (ranging from 1.07 to 1.14 mm) compared with the PD-FS-TSE (ranging from 0.74 to 0.99 mm); however, both morphological sequences showed comparable good results with RMSA of 7.1 to 8.5%. Regarding quantitative T2 mapping, measurements showed T2 relaxation times of about 54 ms with an excellent reproducibility (RMSA) ranging from 3.2 to 4.7%.

Conclusion In our study the assessment of cartilage thickness and T2 relaxation times could be performed with high reproducibility in a clinically realizable scan time, demonstrating new possibilities for further investigations into patient groups.

G. H. Welsch (✉) · S. Trattnig
MR Center, High field MR, Department of Radiology,
Medical University of Vienna,
Lazarettgasse 14,
1090 Vienna, Austria
e-mail: welsch@bwh.harvard.edu

T. C. Mamisch
Department of Orthopaedic Surgery, University of Berne,
Berne, Switzerland

M. Weber
Medical Statistics, Department of Radiology,
Medical University of Vienna,
Vienna, Austria

W. Horger
Siemens Medical Solutions,
Erlangen, Germany

K. Bohndorf
Department of Radiology, Klinikum Augsburg,
Augsburg, Germany

Keywords MRI · Cartilage · Ankle · 3 T · TrueFISP · T2 mapping

Introduction

The exact analysis of articular cartilage in joints with high congruency and a thin cartilage layer is technically demanding [1]. The clinical impact of such an assessment is high since modern surgical therapies require preoperative high-resolution magnetic resonance imaging (MRI) of the ankle joint [2]. Studies on cadaver specimens have shown that MRI is capable of exactly visualizing cartilage

thickness and topography in the ankle at 1.0 and 1.5 Tesla [1, 3, 4]; however, for high-resolution cartilage imaging long scan times detract from clinical application.

The feasibility of 3.0 Tesla MRI in the imaging of small joints with challenging anatomy was demonstrated [5–7] and advances in signal-to-noise-ratio (SNR) with sufficient resolution were shown to improve the staging of osteochondral defects [8].

The importance of advanced coil technology in the visualization of joints with thin cartilage is unquestionable and can be achieved by surface coils or dedicated phased array coils [9, 10]. Combining phased array coils and parallel imaging at 3 T may lead to improved image quality and a reduction in scan time [11, 12].

In isotropic 3D cartilage imaging T1-weighted 3D-FLASH was seen as an adequate sequence [13, 14]. However, recent studies point out that other isotropic 3D gradient echo (GE) sequences show equal or better results [15, 16]. At present with the 3D true fast imaging with steady-state precession (True-FISP) sequence, a steady-state free precession (SSFP) sequence is of increasing importance in providing an isotropic resolution of 0.3 mm within the shortest scan time of all 3D GRE sequences [17].

Besides morphological imaging, biochemical MRI techniques show promising results [18–23] with quantitative T2 as a widely implemented MR parameter to reflect interactions between water molecules and surrounding macromolecules [24].

The aim of the present study was to evaluate the feasibility and reproducibility of high-resolution morphological and biochemical MRI of the articular cartilage of the ankle joint using a new ankle-dedicated phased array coil.

Materials and methods

Patient population

Ten healthy volunteers without known musculoskeletal disease and no history of trauma or pain (24–57 years, mean age 32.4 years, 1 woman, 9 men, mean body mass index 22.3 kg/m²) were included in the study. Ethics approval for this study was provided by the ethics commission of the Medical University, and informed consent was obtained from all patients prior to enrolment in the study.

Imaging parameters

Magnetic resonance imaging was performed on a 3.0 Tesla MR scanner (Magnetom Trio; Siemens Medical Solutions, Erlangen, Germany). A new eight-channel high-resolution, small field of view (FoV) foot and ankle imaging coil was

used (Invivo, Gainesville, FL, USA). This dedicated phased array coil was designed to take advantage of the eight-channel system capabilities, including the parallel imaging application. With its boot design it easily slides down over foot and ankle and can be tilted in 5° increments (Fig. 1). Volunteers were scanned in a supine position, and MRI was performed on the left ankle with the foot at a 90° angle to the lower leg.

All volunteers were scanned once; for variability, evaluation rescanning was achieved in three of the volunteers three times. MRI was carried out after at least half an hour of rest to avoid possible differences in T2 relaxation on behalf of different loading/weight bearing and thus hydration of cartilage prior to MRI. After localizing, a 3D-TrueFISP water excitation sequence was carried out, covering the ankle with 320 isotropic 0.31×0.31×0.31-mm slices using a 160-mm FoV and a 512² matrix. The sequence was optimized for cartilage imaging at 3.0 T taking previous clinical and scientific work and experience into consideration; TR/TE was chosen at 9.65/4.18 ms, Flip angle was 28°, two averages, bandwidth measured 200 Hz/pixel and by utilizing the parallel imaging technique (PAT) with an acceleration factor of 3 using a generalized autocalibrating partially parallel acquisition (GRAPPA) technique, the scan time was set at 9:49 min. All consecutive sequences were planned sagittal to the talar dome using the 3D reconstruction of the isotropic True-FISP images (Fig. 2). One sagittal slice about 5 mm lateral to the medial edge of the talus was used as reference for the following morphological and biochemical imaging. This particular position was chosen as in this area osteochondritis dissecans usually occurs [25]. For the sake of comparability, for all following sequences, in-plane resolution was kept at 0.31×0.31 mm², whereas slice thickness was now set to 3 mm using a 100-mm FoV and a 320² matrix.



Fig. 1 The new dedicated phased array eight-channel, high resolution, small field-of-view (FoV) foot and ankle imaging coil used in this study

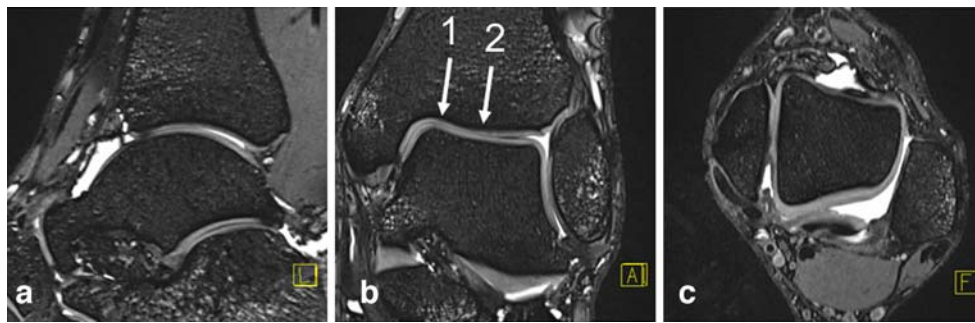


Fig. 2 High-resolution morphological isotropic ($0.31 \times 0.31 \times 0.31$ mm) MRI using the 3D true fast imaging with steady-state precession (True-FISP) sequence. Reconstructed **a** sagittal, **b** coronal, and **c** axial view of the ankle of a healthy volunteer. Further sagittal measurements were

planned on this isotropic sequence and marked by arrows: location 1, 5 mm lateral of the medial border of the talar shoulder; location 2, middle of the talar dome

As a reference in morphological high-resolution imaging of the ankle, in the present study, a proton density fat-suppressed turbo spin-echo (PD-FS-TSE) sequence was performed with TR/TE 2,400/39 ms, a flip angle of 160° , one average, PAT off, bandwidth of 244 Hz/pixel, and 16 slices with a scan time of 4:02 min. Biochemical quantitative T2 imaging was prepared by a multi-echo spin-echo (SE) T2 approach. Using six echoes, the measurement parameters were as follows (TE ~ 16.5, 33.0, 49.5, 66.0, 82.5, 99.0 ms; TR 603 ms; flip angle 180° ; two averages, PAT factor 2 using GRAPPA; bandwidth of 130 Hz/pixel, and 10 slices in 10:53 min). T2 maps were obtained using a pixel-wise, mono-exponential non-negative least squares (NNLS) fit analysis. Quantitative T2 measurements and PD-FS-TSE imaging were conducted in the sagittal direction planned on a 3D view of the isotropic 3D-TrueFISP where a sagittal, coronal, and axial plane is given (Fig. 2). Therefore, 3D-TrueFISP and PD-FS-TSE, as well as T2 mapping, could be assessed in exactly the same plane. Total scanning time with localizing was 28 min.

Data analysis

To evaluate the reproducibility of the measurements, the assessment of cartilage thickness in morphological images

and regions of interest (ROI) for quantitative T2 imaging was done manually by three experts in musculoskeletal MRI. Each analysis was repeated three times at different time points in three different reading sessions. Assessment of cartilage thickness and ROIs for T2 mapping was done by each reader separately; the slices for evaluation had been defined before by all three readers in consensus, saved, and provided identically.

For morphological 3D-TrueFISP and PD-FS-TSE cartilage imaging the cartilage thickness of the trochlear surface of the talus (facing the tibia) and the corresponding inferior articular surface of the tibia (facing the talus) were assessed (Fig. 3). The anatomic regions for cartilage thickness measurements within the two sequences were matched side by side. For quantitative T2 imaging, ROIs within the same regions were evaluated (Fig. 4). Analysis was performed on a multi-modal workstation (Leonardo; Siemens Medical Solutions, Erlangen, Germany) at the maximum magnification. The measurements were obtained from the defined sagittal PD-FS-TSE at the peak of curvature of both articular surfaces starting at the chondral surface border. The vertical line was drawn to the always visible darker borderline to the corresponding cortical bone. Subsequently, the thickness measurements were assessed in an identical positioned plane of the 0.31-mm 3D-TrueFISP

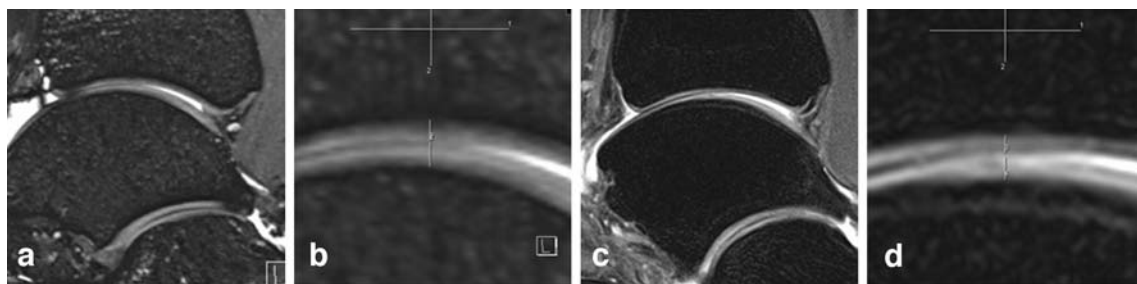


Fig. 3 Measurements were accomplished in **a**, **b** the defined sagittal plane of the 3D-TrueFISP sequence and **c**, **d** the accordingly positioned plane of the proton density fat-suppressed turbo spin echo (PD-FS-TSE) sequence. Starting from the overview (**a**, **c**) for

assessment of cartilage thickness of the articular cartilage of the trochlear surface of the talus, and the corresponding articular cartilage of the inferior surface of the tibia could be evaluated by magnifying the images (**b**, **d**)

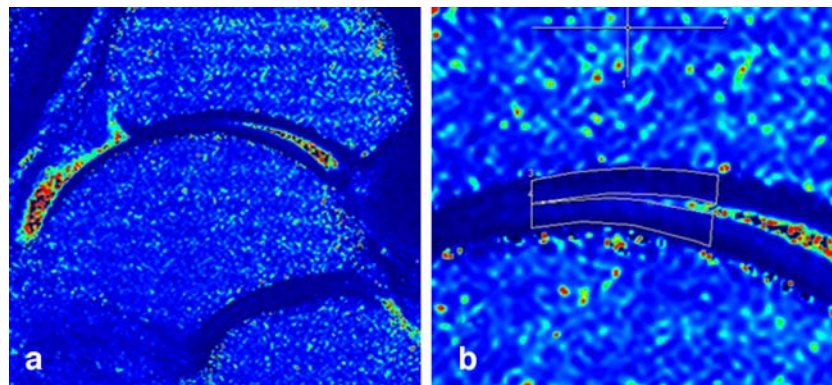


Fig. 4 Quantitative T2 imaging of equally positioned sagittal plane by drawing regions of interest (ROI) within the cartilage layers. **a** Overview and **b** magnified images for evaluation. The vertical line

indicates the peak of curvature, the horizontal line 5 mm in each direction for the repeated ROI measurements

sequence. All measurements were repeated three times by each observer and were accomplished in the defined sagittal plane about 5 mm lateral of the medial border of the talar shoulder where osteochondral defects typically appear (location 1) and in a sagittal plane in the middle of the talar dome in a region of high load-bearing (location 2).

Quantitative T2 measurements were assessed only in location 1. To determine the ROIs for the T2 measurements, at the localization of the thickness measurements at the peak of curvature, the ROIs were drawn 5 mm in each direction. The biochemical assessment (T2 measurements) was achieved in the same location as the morphological thickness measurements (TrueFISP and PD FS TSE); here ROIs of 10 mm in width and the height of the cartilage layer were calculated. The exact pixel size and standard deviation were documented, and the manual segmentation time was limited to 5 min per patient.

Quantitative signal intensity analysis concentrated on image inhomogeneity (non-uniformity, NU). Conventional SNR measurements cannot be reliably assessed for multi-channel coils and parallel imaging because of the inhomogeneous distribution of noise [26]. Assessment was done by a one-acquisition technique where four ROIs were placed within the anatomic structure of interest (cartilage and bone). For identical placement, ROIs were copied from one sequence and pasted onto the remaining ones. NU was defined as $NU = (SD_{ROI}/SI_{ROI}) * 100$; with SI_{ROI} as mean signal intensity of the four ROIs (cartilage or bone) and SD_{ROI} as the mean standard deviation of the respective ROIs [27–29]. Thus, high NU values reflect reduced signal homogeneity; motion artefacts contribute to the NU. Pixel size was kept to 500 pixels for cartilage and 2,500 pixels for bone.

Statistical tests were used to perform the data analyses as follows. Measurements of cartilage thickness and quantitative T2 and NU values were evaluated by analyses of variance using a three-way ANOVA with a random factor, considering the fact of different measurements within each

volunteer. The intra-individual reproducibility was determined as a coefficient of variation (CV, given in percent) for each volunteer, averaged for all volunteers together and was seen as a grade of precision by apportion of standard deviation relating to the mean (intra-individual CV 1). CV was measured for every reader; the average reproducibility was assessed as root mean square average (RMSA, given in percent) [30] of the CVs of all volunteers and all readers. Intra-individual reproducibility was additionally assessed for the repetitive MR measurements of three volunteers (intra-individual CV 2). Furthermore, inter-individual (biological) variability was evaluated (inter-individual CV 3). For significance within CV and RMSA relating to the different sequences, measurements, volunteers, locations, and observers, analysis of variance for correlated data was carried out. SPSS version 15.0 (SPSS Institute, Chicago, IL, USA) for Windows (Microsoft, Redmont, WA, USA) was used, and a p value less than 0.05 was considered statistically significant.

Results

Cartilage thickness

Mean (\pm standard deviation [SD]) cartilage thickness (mm) measurements for two positions within the talocrural joint, for all measurements of all observers, varied between the two morphological sequences. As seen in Table 1, cartilage thickness assessed with the 3D-TrueFISP sequence was significantly higher for all regions than cartilage thickness assessed by the PD-FS-TSE sequence ($p < 0.05$). No significant difference was found between talar and tibial cartilage thickness ($p > 0.05$). However, articular cartilage for location 1 (about 5 mm lateral of the medial border of the talar shoulder) was significantly thicker than that in the middle of the talar dome (location 2; $p < 0.05$).

Table 1 Cartilage thickness (mean \pm SD) at two anatomic points calculated from the 3D true fast imaging with steady-state precession (3D-TrueFISP) sequence and the proton density fat-suppressed turbo spin echo (PD-FS-TSE) sequence

Site	3D-TrueFISP	PD-FS-TSE	<i>p</i> value
Talus (location 1), mm	1.14 \pm 0.23	0.99 \pm 0.28	<0.05
Talus (location 2), mm	1.07 \pm 0.22	0.80 \pm 0.26	<0.05
Tibia (location 1), mm	1.17 \pm 0.21	0.99 \pm 0.28	<0.05
Tibia (location 2), mm	1.08 \pm 0.19	0.74 \pm 0.15	<0.05

p value indicating changes between two different sequences

Quantitative T2 values

Quantitative T2 assessment of hyaline cartilage of the talocrural joint, taking all measurements and all observers together, showed similar results for measurements within the talar and tibial cartilage. Mean T2 values (ms) in articular cartilage of the trochlear surface of the talus were 54.2 \pm 6.9 (ranging from 44 to 72); mean T2 values for articular cartilage of the inferior surface of the tibia were 54.6 \pm 7.2 (ranging from 42 to 77). Mean pixel number for T2 measurements was 416 (ranging from 260 to 635) for talar cartilage and 420 (ranging from 260 to 635) for tibial cartilage.

NU measurements

Signal parameters analyzed using NU showed comparable values for articular cartilage of the talocrural joint with, no significant difference between the 3D-TrueFISP sequence (19.3 \pm 4.0) and the PD-FS-TSE sequence (18.4 \pm 3.4; *p*>0.05). Concerning the surrounding bone, the 3D-TrueFISP sequence showed the significantly lower values of 33.4 \pm 5.2 compared with the PD-FS-TSE sequence, with 50.9 \pm 8.2 (*p*<0.05).

Reproducibility of morphological imaging

Table 2 depicts the results of the reproducibility calculations for the cartilage thickness within the talocrural joint as assessed with the 3D-TrueFISP sequence and the PD-FS-TSE sequence. Both sequences showed similar results for intra-individual reproducibility related to volunteers and raters (CV 1), averaged reproducibility (RMSA), and repetitive measurements (CV 2) with slightly, but not significantly, better results for the 3D-TrueFISP sequence (*p*>0.05). For all locations and both sequences, RMSA ranged from 7.1 to 8.5%. In summary, the intra-individual reproducibility of morphological cartilage thickness measurements showed no significant changes between the 3D-TrueFISP sequence and the PD-

Table 2 Reproducibility values of cartilage thickness measurements calculated from the 3D-TrueFISP sequence and from the PD-FS-TSE sequence

Site		3D-TrueFISP	PD-FS-TSE	<i>p</i> value
Talus (location 1)	CV 1 (%)	5.3–8.6	6.1–9.7	>0.05
	RMSA (%)	7.7	8.2	>0.05
	CV 2 (%)	5.4	5.6	>0.05
Talus (location 2)	CV 3 (%)	20.4	29.0	>0.05
	CV 1 (%)	4.6–8.9	5.3–9.1	>0.05
	RMSA (%)	7.4	7.1	>0.05
Tibia (location 1)	CV 2 (%)	4.7	6.2	>0.05
	CV 3 (%)	20.5	33.3	>0.05
	CV 1 (%)	4.3–10.5	5.9–11.1	>0.05
Tibia (location 2)	RMSA (%)	7.6	8.5	>0.05
	CV 2 (%)	4.2	8.1	>0.05
	CV 3 (%)	17.7	28.5	>0.05
Tibia (location 2)	CV 1 (%)	3.6–11.8	3.6–11.6	>0.05
	RMSA (%)	7.9	8.4	>0.05
	CV 2 (%)	5.6	6.3	>0.05
	CV 3 (%)	17.9	20.3	>0.05

p values indicating changes between the different sequences

CV 1, intra-individual reproducibility for all volunteers (ranged); RMSA, average reproducibility for all volunteers and all readers; CV 2, intra-individual reproducibility concerning repeated measurements in three volunteers; CV 3, inter-individual (biological) variability

FS-TSE sequence (*p*>0.05), relating neither to the four anatomic locations of assessment at the talar and tibial cartilage at location 1 and 2 nor to the three different raters. Concerning the inter-individual (biological) variability (CV 3), values for the 3D-TrueFISP sequence showed significantly lower results compared with those of the PD-FS-TSE sequence (*p*<0.05).

Reproducibility of biochemical imaging

Concerning quantitative T2 measurements, intra-individual reproducibility calculations showed no significant differences between T2 assessment within the cartilage of the trochlear surface of the talus and the cartilage of the inferior surface or the tibia facing to the talus (*p*>0.05). Whereas CV 1 (%) ranged from 2.2 to 4.1 for talar cartilage measurements with an RMSA (%) of 3.2, CV 1 for tibial cartilage ranged from 2.7 to 5.7 with an RMSA of 4.7. Concerning repeated measurements, CV 2 also showed no significant difference between the assessment of talar (ranging from 2.6 to 4.1) and tibial (ranging from 3.0 to 4.7) cartilage. Also, quantitative T2 measurements showed no significant reproducibility changes concerning the three different raters (*p*>0.05). Furthermore, the inter-individual (biological) variability showed comparable results, with 12.8 for talar and 13.3 for tibial cartilage (*p*>0.05).

Discussion

The object of this study was to determine the precision of morphological high resolution isotropic 3D-TrueFISP imaging as well as the feasibility of quantitative T2 within the talocrural joint. To the best of our knowledge this is the first study to evaluate *in vivo* high-resolution ($0.31 \times 0.31 \times 0.31$ mm) TrueFISP imaging and biochemical T2 mapping within the ankle in a clinically acceptable scan-time of about 10 min each.

Magnetic resonance imaging of thin cartilage layers puts challenging demands on imaging techniques. High-field MRI, advanced coil technology, and sophisticated sequences and imaging techniques provide the basis of the imaging protocol used in this study. An improvement in image quality for ankle cartilage pathology was shown by Barr et al. [11] at 3 T compared with 1.5 T. Furthermore, parallel imaging is capable of significantly reducing scan time and may also improve image quality [31]. In a recent article by Bauer et al. [32] using 3 T instead of 1.5 T and the parallel imaging technique, MR images of the ankle were obtained with highly rated diagnostic quality and a scan time reduction of 44%. Whereas this study utilized the common approach of an eight-channel head coil for *in vivo* ankle MRI, in our study a new, anatomically dedicated eight-channel phased array coil, specifically constructed for the ankle, was used. Thus, 3T MRI and parallel imaging prepare the basis of high-resolution morphological and biochemical MR sequences shown in this study.

Concerning morphological cartilage imaging, the reproducibility of thickness measurements was used as a quality criterion. Cartilage thickness within the ankle joint differed between the employed sequences. Existing MR studies on the ankle joint correlated with standard histology showed different results, often underestimating articular cartilage thickness [33, 34]. Taking this fact and recent studies into consideration, the mean cartilage thicknesses in the present study, ranging from 0.74 mm to 0.99 mm, assessed by the PD-FS-TSE, and from 1.07 to 1.17 mm, assessed by the 3D-TrueFISP sequence, are comparable to the findings of Millington et al. [1] and Al-Ali et al. [4]. The higher values measured by the 3D-TrueFISP sequence could be caused by the thinner slices affecting the assessment of cartilage thickness within the curved anatomy of the talocrural joint. Furthermore, the differentiation between hyaline cartilage and the subchondral plate and thus the cartilage thickness measured is dependent on the interpretation of the tidemark of the deep calcified cartilage layer [34]. The varying visualization of the tidemark by different MR sequences may affect the cartilage thickness measured. Partial volume effects as well as chemical shift artefacts, which we tried to reduce by adapting the bandwidth, compound this situation. Hence, a limitation of this study is the lack of histological

comparison. However, differences between the evaluated regions of the medial talar shoulder and the middle of the talar dome could be observed in both sequences. These results agree with the findings of Millington et al. [1], who showed the thickest cartilage occurring over the shoulders of the talus and not at the middle of the talar dome. Concerning the quality of the MRI sequences, reproducibility in multiple measurements is even more important. In our study, the average reproducibility (percent) of cartilage thickness measurements within the ankle joint ranged from 7.4 to 7.9 for the 3D-TrueFISP sequence and from 7.1 to 8.5 for the PD-FS-TSE sequence. The accuracy for both sequences of less than 10% corresponds to or even exceeds that of findings in existing studies on cartilage thickness measurements within the ankle joint [33–35]. The parameters assessed for reproducibility in our study showed slightly better values for the 3D-TrueFISP sequence compared with the PD-FS-TSE. These results imply that the 3D-TrueFISP sequence can be used for the morphological evaluation of cartilage thickness. Additionally, its isotropic dataset of $0.31 \times 0.31 \times 0.31$ mm allows reconstruction in multiple planes, angulation, and thus visualization of other important anatomical structures within the hind foot. Whereas in available sequences used for high-resolution MRI of the ankle, slice thickness is set to 3–4 mm [9, 36] or scan time is up to 20 min [1, 4], the presented 3D-TrueFISP sequence facilitates high-resolution isotropic MRI in less than 10 min. Furthermore, NU values showed comparable results for articular cartilage within both sequences, and with regard to the surrounding bone even more homogeneous results for 3D-TrueFISP. Recommendation of the 3D-TrueFISP sequence for its potential improvement in high-resolution cartilage assessment of the patella [17] can, according to the present study, also be suggested for the thin cartilage layers within the ankle joint.

The ability to obtain information regarding ultrastructural organization of cartilage from MRI is highly desirable. T2 relaxation times can be regarded as accepted values for the biochemical evaluation of relatively thick articular cartilage within the knee in diverse studies [24, 37–41]. The ankle joint, with its thin cartilage layers, remains a challenge in quantitative T2 mapping. In the present study we proved the feasibility and high reproducibility of this technique within the ankle. Mean T2 values of around 54 ms found in articular cartilage of the talocrural joint are comparable with those described for healthy cartilage within the femorotibial joint [41]. Mean reproducibility (percent) for repeated T2 measurements even exceeded morphological thickness evaluation. T2 relaxation times have been shown in different studies to be sensitive for cartilage alterations, as seen in osteoarthritis [42–45] or after surgical cartilage repair procedures [21, 22, 38, 46]. Subsequently, quantitative T2 mapping may accomplish the evaluation of ankle joint

pathologies such as OCD, or may be valuable in the follow-up of demanding surgical techniques like matrix-associated chondrocyte implantation [47–50]. The limitation of the manually assessed thickness and T2 values in this volunteer study may provide the basis for further evaluation of cartilage repair tissue within the ankle.

In our study, defined regions within the thin and demanding cartilage of the talocrural joint were analyzed and an assessment of cartilage thickness and T2 relaxation was performed in a clinically acceptable scanning time. The results obtained show a good reproducibility of high-resolution isotropic 3D-TrueFISP, PD-FS-TSE, and quantitative T2 cartilage imaging providing an excellent basis for diagnosis, grading, and follow-up of pathological conditions of the ankle cartilage layers.

References

1. Millington SA, Li B, Tang J, et al. Quantitative and topographical evaluation of ankle articular cartilage using high resolution MRI. *J Orthop Res* 2007; 25: 143–151.
2. Hangody L, Fules P. Autologous osteochondral mosaicplasty for the treatment of full-thickness defects of weight-bearing joints: ten years of experimental and clinical experience. *J Bone Joint Surg Am* 2003; 85–A(Suppl 2): 25–32.
3. Ba-Ssalamah A, Schibany N, Puig S, Herneth AM, Noebauer-Huhmann IM, Trattnig S. Imaging articular cartilage defects in the ankle joint with 3D fat-suppressed echo planar imaging: comparison with conventional 3D fat-suppressed gradient echo imaging. *J Magn Reson Imaging* 2002; 16: 209–216.
4. Al-Ali D, Graichen H, Faber S, Englmeier KH, Reiser M, Eckstein F. Quantitative cartilage imaging of the human hind foot: precision and inter-subject variability. *J Orthop Res* 2002; 20: 249–256.
5. Bolog N, Nanz D, Weishaupt D. Musculoskeletal MR imaging at 3.0 T: current status and future perspectives. *Eur Radiol* 2006; 16: 1298–1307.
6. Mosher TJ. Musculoskeletal imaging at 3T: current techniques and future applications. *Magn Reson Imaging Clin N Am* 2006; 14: 63–76.
7. Ramnath RR. 3T MR imaging of the musculoskeletal system. II. Clinical applications. *Magn Reson Imaging Clin N Am* 2006; 14: 41–62.
8. Schibany N, Ba-Ssalamah A, Marlovits S, et al. Impact of high field (3.0 T) magnetic resonance imaging on diagnosis of osteochondral defects in the ankle joint. *Eur J Radiol* 2005; 55: 283–288.
9. Antonio GE, Griffith JF, Yeung DK. Small-field-of-view MRI of the knee and ankle. *AJR Am J Roentgenol* 2004; 183: 24–28.
10. Eckstein F, Kunz M, Hudelmaier M, et al. Impact of coil design on the contrast-to-noise ratio, precision, and consistency of quantitative cartilage morphometry at 3 Tesla: a pilot study for the osteoarthritis initiative. *Magn Reson Med* 2007; 57: 448–454.
11. Barr C, Bauer JS, Malfair D, et al. MR imaging of the ankle at 3 Tesla and 1.5 Tesla: protocol optimization and application to cartilage, ligament and tendon pathology in cadaver specimens. *Eur Radiol* 2007; 17: 1518–1528.
12. Ramnath RR. 3T MR imaging of the musculoskeletal system. I. Considerations, coils, and challenges. *Magn Reson Imaging Clin N Am* 2006; 14: 27–40.
13. Burgkart R, Glaser C, Hyhlik-Durr A, Englmeier KH, Reiser M, Eckstein F. Magnetic resonance imaging-based assessment of cartilage loss in severe osteoarthritis: accuracy, precision, and diagnostic value. *Arthritis Rheum* 2001; 44: 2072–2077.
14. Glaser C, Faber S, Eckstein F, et al. Optimization and validation of a rapid high-resolution T1-w 3D FLASH water excitation MRI sequence for the quantitative assessment of articular cartilage volume and thickness. *Magn Reson Imaging* 2001; 19: 177–185.
15. Eckstein F, Hudelmaier M, Wirth W, et al. Double echo steady state magnetic resonance imaging of knee articular cartilage at 3 Tesla: a pilot study for the Osteoarthritis Initiative. *Ann Rheum Dis* 2006; 65: 433–441.
16. Friedrich KM, Reiter G, Kaiser B, et al. Cartilage imaging: fundamental evaluation of modern high-resolution isotropic 3D MR sequences at 3 T. *Eur Radiol* 2007; 17.
17. Weckbach S, Mendlik T, Horger W, Wagner S, Reiser MF, Glaser C. Quantitative assessment of patellar cartilage volume and thickness at 3.0 tesla comparing a 3D-fast low angle shot versus a 3D-true fast imaging with steady-state precession sequence for reproducibility. *Invest Radiol* 2006; 41: 189–197.
18. Burstein D, Velyvis J, Scott KT, et al. Protocol issues for delayed Gd(DTPA)(2-)-enhanced MRI: (dGEMRIC) for clinical evaluation of articular cartilage. *Magn Reson Med* 2001; 45: 36–41.
19. Miller KL, Hargreaves BA, Gold GE, Pauly JM. Steady-state diffusion-weighted imaging of in vivo knee cartilage. *Magn Reson Med* 2004; 51: 394–398.
20. Trattnig S, Millington SA, Szomolanyi P, Marlovits S. MR imaging of osteochondral grafts and autologous chondrocyte implantation. *Eur Radiol* 2007; 17: 103–118.
21. Watrin-Pinzano A, Ruau JP, Cheli Y, et al. Evaluation of cartilage repair tissue after biomaterial implantation in rat patella by using T2 mapping. *Magma* 2004; 17: 219–228.
22. White LM, Sussman MS, Hurtig M, Probyn L, Tomlinson G, Kandel R. Cartilage T2 assessment: differentiation of normal hyaline cartilage and reparative tissue after arthroscopic cartilage repair in equine subjects. *Radiology* 2006; 241: 407–414.
23. Williams A, Gillis A, McKenzie C, et al. Glycosaminoglycan distribution in cartilage as determined by delayed gadolinium-enhanced MRI of cartilage (dGEMRIC): potential clinical applications. *Am J Roentgenol* 2004; 182: 167–172.
24. Glaser C. New techniques for cartilage imaging: T2 relaxation time and diffusion-weighted MR imaging. *Radiol Clin North Am* 2005; 43: 641–653.
25. Steinhagen J, Niggemeyer O, Bruns J. [Etiology and pathogenesis of osteochondrosis dissecans tali]. *Orthopade* 2001; 30: 20–27.
26. Dietrich O, Raya JG, Reeder SB, Reiser MF, Schoenberg SO. Measurement of signal-to-noise ratios in MR images: influence of multichannel coils, parallel imaging, and reconstruction filters. *J Magn Reson Imaging* 2007; 26: 375–385.
27. Firbank MJ, Coulthard A, Harrison RM, Williams ED. A comparison of two methods for measuring the signal to noise ratio on MR images. *Phys Med Biol* 1999; 44: N261–N264.
28. Li T, Mirowsitz SA. Fast multi-planar gradient echo MR imaging: impact of variation in pulse sequence parameters on image quality and artifacts. *Magn Reson Imaging* 2004; 22: 807–814.
29. Noebauer-Huhmann IM, Glaser C, Dietrich O, et al. MR imaging of the cervical spine: assessment of image quality with parallel imaging compared to non-accelerated MR measurements. *Eur Radiol* 2007; 17: 1147–1155.
30. Gluer CC, Blake G, Lu Y, Blunt BA, Jergas M, Genant HK. Accurate assessment of precision errors: how to measure the reproducibility of bone densitometry techniques. *Osteoporos Int* 1995; 5: 262–270.
31. Blaimer M, Breuer F, Mueller M, Heidemann RM, Griswold MA, Jakob PM. SMASH, SENSE, PILS, GRAPPA: how to choose the optimal method. *Top Magn Reson Imaging* 2004; 15: 223–236.

32. Bauer JS, Banerjee S, Henning TD, Krug R, Majumdar S, Link TM. Fast high-spatial-resolution MRI of the ankle with parallel imaging using GRAPPA at 3 T. *AJR Am J Roentgenol* 2007; 189: 240–245.
33. Tan TC, Wilcox DM, Frank L, et al. MR imaging of articular cartilage in the ankle: comparison of available imaging sequences and methods of measurement in cadavers. *Skeletal Radiol* 1996; 25: 749–755.
34. Trattnig S, Breitenseher MJ, Huber M, et al. [Determination of cartilage thickness in the ankle joint. an MRT (1.5)-anatomical comparative study]. *Rofo* 1997; 166: 303–306.
35. Eckstein F, Reiser M, Englmeier KH, Putz R. In vivo morphometry and functional analysis of human articular cartilage with quantitative magnetic resonance imaging—from image to data, from data to theory. *Anat Embryol (Berl)* 2001; 203: 147–173.
36. Mintz DN, Tashjian GS, Connell DA, Deland JT, O'Malley M, Potter HG. Osteochondral lesions of the talus: a new magnetic resonance grading system with arthroscopic correlation. *Arthroscopy* 2003; 19: 353–359.
37. Dardzinski BJ, Mosher TJ, Li S, Van Slyke MA, Smith MB. Spatial variation of T2 in human articular cartilage. *Radiology* 1997; 205: 546–550.
38. Kurkijarvi JE, Nissi MJ, Ojala RO, et al. In vivo T2 mapping and dGEMRIC of human articular cartilage repair after autologous chondrocyte transplantation. *Proc Intl Soc Magn Reson Med* 2005; 13: 481.
39. Mosher TJ, Dardzinski BJ, Smith MB. Human articular cartilage: influence of aging and early symptomatic degeneration on the spatial variation of T2—preliminary findings at 3 T. *Radiology* 2000; 214: 259–266.
40. Mosher TJ, Smith H, Dardzinski BJ, Schmithorst VJ, Smith MB. MR imaging and T2 mapping of femoral cartilage: in vivo determination of the magic angle effect. *AJR Am J Roentgenol* 2001; 177: 665–669.
41. Mosher TJ, Smith HE, Collins C, et al. Change in knee cartilage T2 at MR imaging after running: a feasibility study. *Radiology* 2005; 234: 245–249.
42. Dunn TC, Lu Y, Jin H, Ries MD, Majumdar S. T2 relaxation time of cartilage at MR imaging: comparison with severity of knee osteoarthritis. *Radiology* 2004; 232: 592–598.
43. Koff MF, Amrami KK, Kaufman KR. Clinical evaluation of T2 values of patellar cartilage in patients with osteoarthritis. *Osteoarthritis Cartilage* 2007; 15: 198–204.
44. Link TM, Stahl R, Woertler K. Cartilage imaging: motivation, techniques, current and future significance. *Eur Radiol* 2007; 17: 1135–1146.
45. Mosher TJ, Dardzinski BJ. Cartilage MRI T2 relaxation time mapping: overview and applications. *Semin Musculoskelet Radiol* 2004; 8: 355–368.
46. Welsch GH, Mamisch TC, Salomonowitz E, et al. Quantitative T2 mapping of matrix-associated autologous chondrocyte transplantation: an in vivo follow-up study. *Eur Radiol* 2007; 17: 291.
47. Dorotka R, Kotz R, Trattnig S, Nehrer S. [Mid-term results of autologous chondrocyte transplantation in knee and ankle. A one- to six-year follow-up study]. *Z Rheumatol* 2004; 63: 385–392.
48. Giannini S, Buda R, Grigolo B, Vannini F, De Franceschi L, Facchini A. The detached osteochondral fragment as a source of cells for autologous chondrocyte implantation (ACI) in the ankle joint. *Osteoarthritis Cartilage* 2005; 13: 601–607.
49. Gigante A, Bevilacqua C, Ricevuto A, Mattioli-Belmonte M, Greco F. Membrane-seeded autologous chondrocytes: cell viability and characterization at surgery. *Knee Surg Sports Traumatol Arthrosc* 2007; 15: 88–92.
50. Koulalis D, Schultz W, Heyden M. Autologous chondrocyte transplantation for osteochondritis dissecans of the talus. *Clin Orthop Relat Res* 2002; 395: 186–192.